

Morphologic Characterization of Anodic Titania Nanotube Arrays for Dye-Sensitized Solar Cells

Lu-Lin Li^a (李陸玲), Chiau-Yiag Tsai^a (蔡喬盈), Hui-Ping Wu^a (吳慧屏),
Chien-Chon Chen^{b,*} (陳建仲) and Eric Wei-Guang Diau^{a,*} (刁維光)

^aDepartment of Applied Chemistry and Institute of Molecular Science, National Chiao Tung University,
Hsinchu 30010, Taiwan, R.O.C.

^bDepartment of Energy and Resources, National United University, Miaoli 36003, Taiwan, R.O.C.

We report morphologic characterization of the anodic titanium oxide (ATO) films with highly-ordered titania (TiO₂) nanotube (NT) arrays grown perpendicularly to a titanium (Ti) foil. The length of the ATO arrays was controlled by various electrolytes and anodic periods at a constant applied voltage. In order to enhance the pathways for electron percolation, the ATO film was annealed in an air furnace, forming anatase TiO₂. After TiCl₄ post-treatment to enhance the ruthenium-based dye loading on the ATO surface, the optimized ATO arrays were used as a photoanode in a dye-sensitized solar cell (DSSC). The best performance of the NT-DSSC device was achieved with a NH₄F-based ATO film at length of 15 μm, giving $J_{SC} = 12.15 \text{ mA cm}^{-2}$, $V_{OC} = 0.74 \text{ V}$, $FF = 0.69$, and $\eta = 6.2\%$ under backside illumination.

Keywords: ATO; TiO₂; Nanotube; Anodization; DSSC.

INTRODUCTION

Titania (TiO₂) has been used in various applications, such as environmental applications,¹ catalysis,² dielectrics,³ optoelectronics,⁴ sensors,⁵ and solar cells.⁶ Among three stable phases (anatase, brookite and rutile) of titanium dioxide, the anatase TiO₂ has photoelectric, photocatalytic, and hydrophilic characteristics, which are applied in solar cells, disinfection, and surface self-cleaning applications.⁷ Since the report of a low-cost dye-sensitized solar cell (DSSC) in 1991 by O'Regan and Grätzel,⁸ the DSSC has been regarded as a promising candidate for next-generation solar cells.⁹ The electron-collecting layer (photoanode) of a conventional DSSC is composed of randomly packed TiO₂ nanoparticles (NP). With sunlight irradiation from the transparent anode (front illumination), the best photovoltaic power conversion efficiency (η) of a NP-DSSC device has reached $\eta \sim 11\%$.¹⁰⁻¹² The great advantage of NP-DSSC is the large surface area of the nanoporous TiO₂ films for dye adsorption. However, it has been pointed out that the trap-limited diffusion for electron transport in NP-DSSC is a limiting factor in achieving higher cell performance.¹³

To improve the charge-collection efficiency by promoting faster electron transport and slower charge recombination, several different methods with TiO₂ films constructed of oriented one-dimensional (1D) nanostructures have been established. For example, DSSCs based on 1D TiO₂ nanowires (NW)¹⁴ have yielded a cell performance of $\eta = 5.0\%$ under front-side illumination.¹⁵ Alternatively, TiO₂ nanotubes (NT) have been synthesized using the sol-gel¹⁶ and the potentiostatic anodization¹⁷ methods. In our previous report,¹⁸ we produced ATO arrays with length of 19 μm in ethylene glycol (EG) electrolyte containing 0.5% NH₄F at 60 V for 3 h. The cell performances of the corresponding NT-DSSC devices attained $\eta \sim 7\%$ with TiCl₄ post-treatment under rear illumination.

Anodization is an efficient method to fabricate TiO₂ nanotube arrays. This process uses fluoride-based electrolyte solutions such as HF or KF-based aqueous solution and NH₄F-based non-aqueous solutions. With these electrolytes, the ATO length can be controlled to the ranges of 0.3 to 0.5 μm (HF), 1.5 to 5 μm (KF), and 10 to 18 μm (NH₄F). Besides, the morphology of these nanotubes can also be controlled by using different fluoride-based elec-

Special Issue for the 2009 International Symposium of Dye-Sensitized Solar Cells

* Corresponding author. (a)Tel: +886-3-5131524; Fax: +886-3-5723764; E-mail: diau@mail.nctu.edu.tw (EWGD);

(b) Tel: +886-37-381836; Fax: +886-37-381237; E-mail: ccchen@nuu.edu.tw (CCC).

trollyte solutions. This study presents a simple and inexpensive process for direct formation of ATO NT on recyclable conductive material of Ti as a photoanode of DSSC that allows production of a flexible electrode with large active area.

EXPERIMENT

Fabrication of ATO arrays

An ordered channel-array of anodic titanium oxide was fabricated by anodizing Ti foil (Aldrich, 99.7% purity) about a thickness of 127 μm and 10 cm^2 in size. A two-electrode cell, composed of platinum (Pt) sheet (2 cm^2) as the cathode and Ti foil as the working electrode, was used during the anodization at 25 $^\circ\text{C}$. The varied ATO lengths of 0.5, 2.0, 3.5, and 18 μm were produced using electrolyte containing potassium fluoride anhydrous (KF, 99.9%), 13.8 wt.% sodium bisulfate ($\text{NaHSO}_4 \cdot 2\text{H}_2\text{O}$, 99.9%) and 5.9 wt.% trisodium citrate dihydrate ($\text{Na}_3\text{C}_6\text{H}_5\text{O}_7 \cdot 2\text{H}_2\text{O}$) solution at 25 V for 1, 4, 6 and 17 h, respectively. Alternatively, the ATO films with well-ordered arrays were produced in electrolyte (pH = 6.4) containing ammonium fluoride (NH_4F , 99.9%, 0.25 wt%) and H_2O (2 vol%) in ethylene glycol (EG) at 60V. After the anodization, the ATO film was washed in ethanol, and annealed at 450 $^\circ\text{C}$ for 1 h to crystallize amorphous TiO_2 into its anatase phase. The micro-morphology and composition of ATO were determined with a JEOL 6500 scanning electron microscope (SEM). The details of the morphology and crystal structure of the ATO were observed using a JEOL 2000 transmission electron microscope (TEM).

Cell Fabrication and characterization

For photovoltaic device studies, a TiCl_4 post-treatment was performed on the ATO arrays to increase the surface area. The ATO films were first immersed in a 0.2 M TiCl_4 solution for 1 h at 70 $^\circ\text{C}$, rinsed in ethanol, and annealed in air at 400 $^\circ\text{C}$ for 30 min. Then the electrode was soaked in a solution of 5×10^{-4} M $\text{RuL}_2(\text{NCS})_2$ (N3 dye) in ethanol for 12 h. A transparent conducting oxide (TCO) coated with 10 nm of Pt by sputtering was used as the counter electrode, and the device was simply sealed with a hot-melt film (SX1170, Solaronix, thickness of 25 μm). Then the electrolyte containing lithium iodide (LiI, 0.1 M), diiodine (I_2 , 0.01 M), 4-*tert*-butylpyridine (TBP, 0.5 M), butyl methyl imidazolium iodide (BMII, 0.6 M), and guanidinium thiocyanate (GuNCS, 0.1 M) in a mixture of acetonitrile (CH_3CN , 99.9%) and valeronitrile (*n*- $\text{C}_4\text{H}_9\text{CN}$, 99.9%) (v/v = 85/15) was introduced into the space be-

tween the two electrodes. The cell performance was characterized on the back side illumination with an active illuminated area of 0.28 cm^2 by mask on the transparent counter electrode.¹⁹ Measurements of *IV* curves were made with a digital source meter (Keithley 2400, computer-controlled) with the device under one-sun AM-1.5 irradiation from a solar simulator (Newport-Oriel 91160) calibrated with a Si-based reference cell (Hamamatsu S1133) containing an IR-cut filter (KG5) to correct the spectral mismatch of the lamp.²⁰

RESULTS AND DISCUSSION

Fabrication and characterization of ATO arrays

The anodization was performed using KF-based and NH_4F -based electrolyte solutions to investigate the morphology of the ATO arrays affecting by these electrolytes. Fig. 1 presents top and cross-section views of (a) SEM and (b) TEM micrograph images of ATO arrays anodized in electrolyte solution containing 0.58 wt.% KF, 13.8 wt.% $\text{NaHSO}_4 \cdot 2\text{H}_2\text{O}$ and 5.9 wt.% $\text{Na}_3\text{C}_6\text{H}_5\text{O}_7 \cdot 2\text{H}_2\text{O}$ at 25 V for 6 h. Fig. 1a shows the nano-channels and pores with a diameter of 100 nm and a 25 nm-thick pore wall. The KF-based ATO shows more separated and disordered features compared to its NH_4F -based counterpart. The inter-pore distance is about 120 nm, leading to a pore density of 8×10^9 pores/ cm^2 and a porosity of 68.2%. From the TEM image shown in Fig. 1b, the ATO pore size was determined to be ~ 100 nm, and the pore wall of ~ 20 nm. We found that the length of ATO NT increased as anodization period increased. However, a thicker ATO film results in weaker adherence of the ATO film on the Ti substrate. We produced four anodic ATO NT films with various tube lengths of 0.5, 2, 3.5 and 18 μm via anodization with time of 1, 4, 6 and 17, respectively. The corresponding side-view SEM images are shown in Fig. 2a-d.

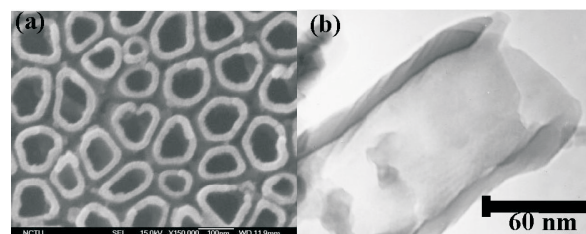


Fig. 1. (a) SEM and (b) TEM images of anodic TiO_2 nanotube arrays formed in 0.58 wt.% KF+13.8 wt.% $\text{NaHSO}_4 \cdot 2\text{H}_2\text{O}$ + 5.9 wt.% $\text{Na}_3\text{C}_6\text{H}_5\text{O}_7 \cdot 2\text{H}_2\text{O}$ solution at 25V for 6 r.

Different from KF-based ATO arrays, the SEM images (Fig. 3) of NH₄F-based ATO arrays, formed in 0.5 wt.% NH₄F + EG electrolyte at 60V for 10 h, presents an ordered nanochannel structures. Fig. 3 shows (a) top view of ordered pores with 120 nm pore diameter and 25 nm wall thickness, (b) bottom view of a hexagonal compact barrier layer, (c) cross-section view of straight tube, with open pores at the top of the tube, but closed pores on the tube bottom, and (d) a tube length of 15 μ m.

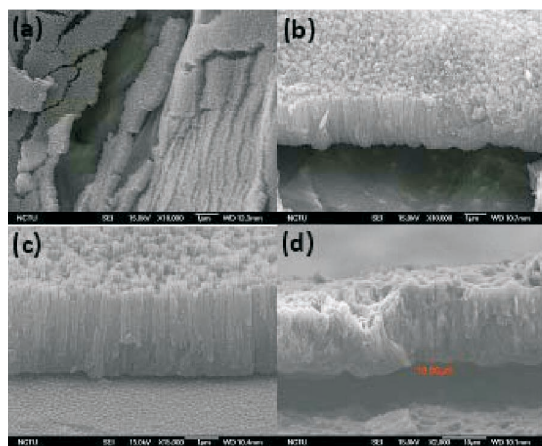


Fig. 2. SEM images of anodic TiO₂ nanotubes showing the cross-section views of ATO at various anodization periods. Anodic times of 1, 4, 6, and 17 r resulted in tube lengths of (a) 0.5 μ m, (b) 2 μ m, (c) 3.5 μ m, and (d) 18 μ m.

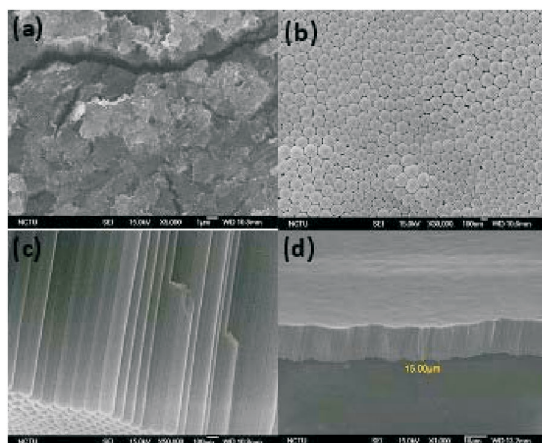


Fig. 3. SEM images of ATO structures formed in 0.5 wt.% NH₄F + EG electrolyte at 60V for 10 hr. (a) Top view of ordered pores, (b) bottom view of compact barrier layer, (c) cross-section view of straight tube, and (d) side-view at a large scale showing the thickness of 15 μ m.

Photovoltaic performance on TiCl₄ post-treated ATO Films

Before the fabrication of devices, the ATO photoanodes were treated with TiCl₄ to produce TiO₂ nanoparticles on the surface of TiO₂ nanotubes. These particles also formed on the areas of the substrate which was not covered with TiO₂ NT arrays. Therefore, the TiCl₄ post-treatment not only increases the surface area for dye-loading but also enhances the V_{OC} by preventing the contact between electrode and electrolyte. Fig. 4 shows SEM images of the ATO before and after TiCl₄ treatment. The original ATO film (Fig. 4a, top view; Fig. 4b, side view) was smooth and clean before TiCl₄ treatment. However, after TiCl₄ treatment, TiO₂ nanoparticles were formed on the surface (Fig. 4c, top view; Fig. 4d, side view) which increases the roughness of the surface. A rough surface will enhance the dye-loading amounts of the ATO film. Fig. 5 shows TEM

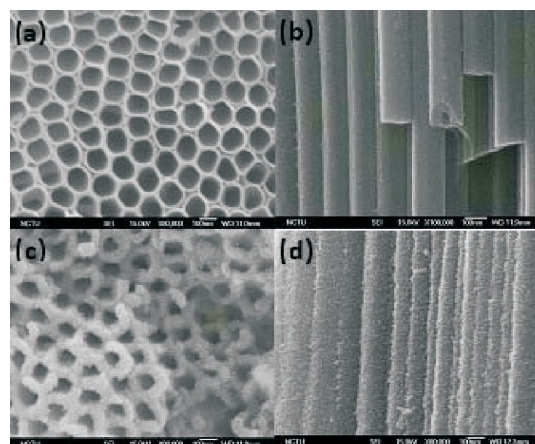


Fig. 4. The SEM images of original ATO films before TiCl₄ treatment showing (a) the tube surface and (b) the tube wall being smooth and clean. After the ATO films soaking in 0.02M TiCl₄ solution at 70 $^{\circ}$ C for 1 h, roughness appeared: (c) top view and (d) side view of the tubes.

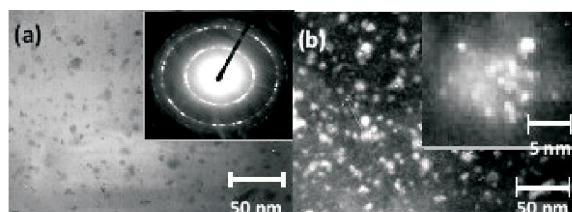


Fig. 5. The TEM images of N3 dye on the copper grid; (a) bright field; (b) dark field, in which white points represent the N3 dye molecules.

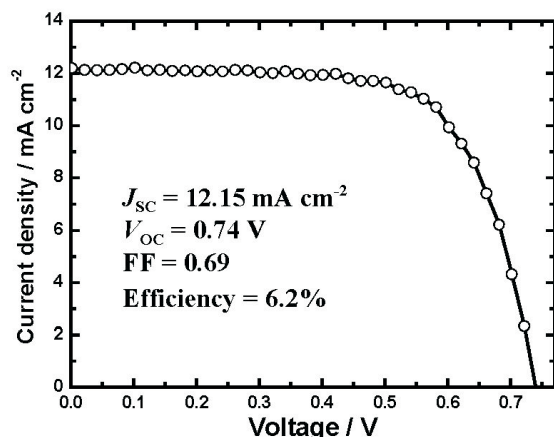


Fig. 6. Current-voltage characteristics of the NH_4F -based NT-DSSC devices with TiCl_4 post-treatment under simulated AM 1.5 solar illumination at 100 mW cm^{-2} with active area of 0.28 cm^2 .

images of TiO_2 nanotubes after N3 dye immersion for 4 hours. The dark field image (a) and diffraction pattern (b) indicated that N3 dye molecules (white) were attached on the tube wall.

The N3/ATO films were fabricated into NT-DSSC devices of which the corresponding IV curves are shown in Fig. 6. The photovoltaic performance exhibits that the current density at short circuit (J_{SC} in mA cm^{-2}) is 12.15, the voltage at open circuit (V_{OC} in V) is 0.74, the fill factor (FF) is 0.69, giving the efficiency of power conversion ($\eta = J_{\text{SC}} \cdot V_{\text{OC}} \cdot \text{FF} / P_{\text{in}}$ with $P_{\text{in}} = 100 \text{ mW cm}^{-2}$) to be 6.2%.

CONCLUSIONS

In this study, we present a simple anodic process for direct formation of ATO on a Ti foil as a DSSC anode. By varying the fluoride-based electrolyte solution, KF and NH_4F , and anodization period, an ATO film with vertically oriented NT arrays was produced. The performance of the optimized NT-DSSC device was achieved with a NH_4F -based ATO film at length of $15 \mu\text{m}$, showing a power conversion efficiency of 6.2%.

ACKNOWLEDGEMENT

National Science Council of Taiwan and the MOE-ATU program provided financial support.

Received December 8, 2009.

REFERENCES

1. Quan, X.; Yang, S.; Ruan, X.; Zhao, H. *Environ. Sci. Technol.* **2005**, *39*, 3770.
2. Yu, Y.; Yu, J. C.; Kwok, Y.; Che, Y.; Zhao, J.; Ding, L.; Ge, W.; Qong, P. *Appl. Catal. A* **2005**, *289*, 189.
3. Tatarenko, N. I.; Mozalev, A. *Solid State Electron.* **2001**, *45*, 1009.
4. Tun, Z.; Noel, J. J.; Shoesmith, D. W. *J. Electrochem. Soc.* **1999**, *146*, 988.
5. Varghese, O. K.; Mor, G. K.; Grimes, C. A.; Paulose, M.; Mukherjee, N. *J. Nanosci. Nanotechnol.* **2004**, *4*, 733.
6. Mor, G. K.; Shankar, K.; Paulose, M.; Varghese, O. K.; Grimes, C. A. *Nano Lett.* **2006**, *6*, 215.
7. Chen, C.-C.; Lin, J.-S.; Diao, E. W.-G.; Liu, T.-F. *Appl. Phys. A* **2008**, *92*, 615.
8. O'Regan, B.; Grätzel, M. *Nature* **1991**, *353*, 737.
9. Grätzel, M. *Nature* **2001**, *414*, 338.
10. Nazeeruddin, M. K.; Angelis, F. D.; Fantacci, S.; Selloni, A.; Viscardi, G.; Liska, P.; Ito, S.; Takeru, B.; Grätzel, M. *J. Am. Chem. Soc.* **2005**, *127*, 16835.
11. Wei, M.; Konishi, Y.; Zhou, H.; Yanagida, M.; Sugihara, H.; Arakawa, H. *J. Mater. Chem.* **2006**, *16*, 1287.
12. Koide, N.; Islam, A.; Chiba, Y.; Han, L. *J. Photochem. Photobiol. A* **2006**, *182*, 296.
13. (a) Law, M.; Greene, L. E.; Johnson, J. C.; Saykally, R.; Yang, P. *Nat. Mater.* **2005**, *4*, 455; (b) Zhu, K.; Neale, N. R.; Miedaner, A.; Frank, A. J. *Nano Lett.* **2007**, *7*, 69.
14. Song, M. Y.; Kim, D. K.; Ihn, K. J.; Jo, S. M.; Kim, D. Y. *Nanotechnology* **2004**, *15*, 1861.
15. Cheung, K. Y.; Yip, C. T.; Djurišić, A. B.; Leung, Y. H.; Chan, W. K. *Adv. Funct. Mater.* **2007**, *17*, 555.
16. Mor, G. K.; Shankar, K.; Paulose, M.; Varghese, O. K.; Grimes, C. A. *Nano Lett.* **2006**, *6*, 215.
17. Chiba, Y.; Islam, A.; Watanabe, Y.; Komiya, R.; Koide, N.; Han, L. *Jpn. J. Appl. Phys.* **2006**, *45*, L638.
18. Chen, C.-C.; Chung, H.-W.; Chen, C.-H.; Lu, H.-P.; Lan, C.-M.; Chen, S.-F.; Luo, L.; Hung, C.-S.; and Diao, E. W.-G. *J. Phys. Chem. C* **2008**, *112*, 19151.
19. Ito, S.; Nazeeruddin, M. K.; Liska, P.; Comte, P.; Charvet, R.; Pe'chy, P.; Jirousek, M.; Kay, A.; Zakeeruddin, S. M.; and Grätzel, M. *Prog. Photovolt.: Res. Appl.* **2006**, *14*, 589.
20. Ito, S.; Matsui, H.; Okada, K.; Kusano, S.; Kitamura, T.; Wada, Y.; Yanagida, S. *Sol. Energy Mater. Sol. Cells* **2004**, *82*, 421.